Supplementary Information

DNA damaging, cell cytotoxicity and serum albumin binding efficacy of the rutin-Cu(II) complex

Atanu Singha Roy[†,#,*], Debi Ranjan Tripathy[†], Sintu Samanta[‡], Sudip K. Ghosh[‡] and Swagata Dasgupta[†]

[†]Department of Chemistry, Indian Institute of Technology, Kharagpur 721302, India

[‡]Department of Biotechnology, Indian Institute of Technology, Kharagpur 721302, India

[#]Present address: Department of Chemistry, National Institute of Technology, Meghalaya, Shillong 793003, India

1. Synthesis and characterization of the rutin-Cu(II) complex

The procedure of synthesis and characterization of the rutin-Cu(II) complex has been described in the supplementary section of our recent publication.[1] The polyphenol to Cu(II) ratio estimated from the Job's plot based on UV-vis study is also provided in the same. The mass spectra (LRMS-ESI+) of the rutin-Cu(II) complex has been presented in Figure S1. The mass of the complex is m/z 1318.37 for M^+ and 1319.60 for ($M+H^+$) respectively, which supports the 2:1 rutin to Cu(II) ratio as obtained from the Job's method. The energy-optimized structure of the rutin-Cu(II) complex has been generated using density functional theory with the help of DMol3 (Figure 1). The DNP basis set with BLYP functional has been employed for the geometric optimization keeping the effective core potential on copper.[2]

References

1. D. R. Tripathy, A. Singha Roy, S. Dasgupta, *FEBS Lett.*, 2011, 585, 3270–3276.
2. K. S. Ghosh, B. K. Sahoo, D. Jana, S. Dasgupta, *J. Inorg. Biochem.*, 2008, 102, 1711–1718.

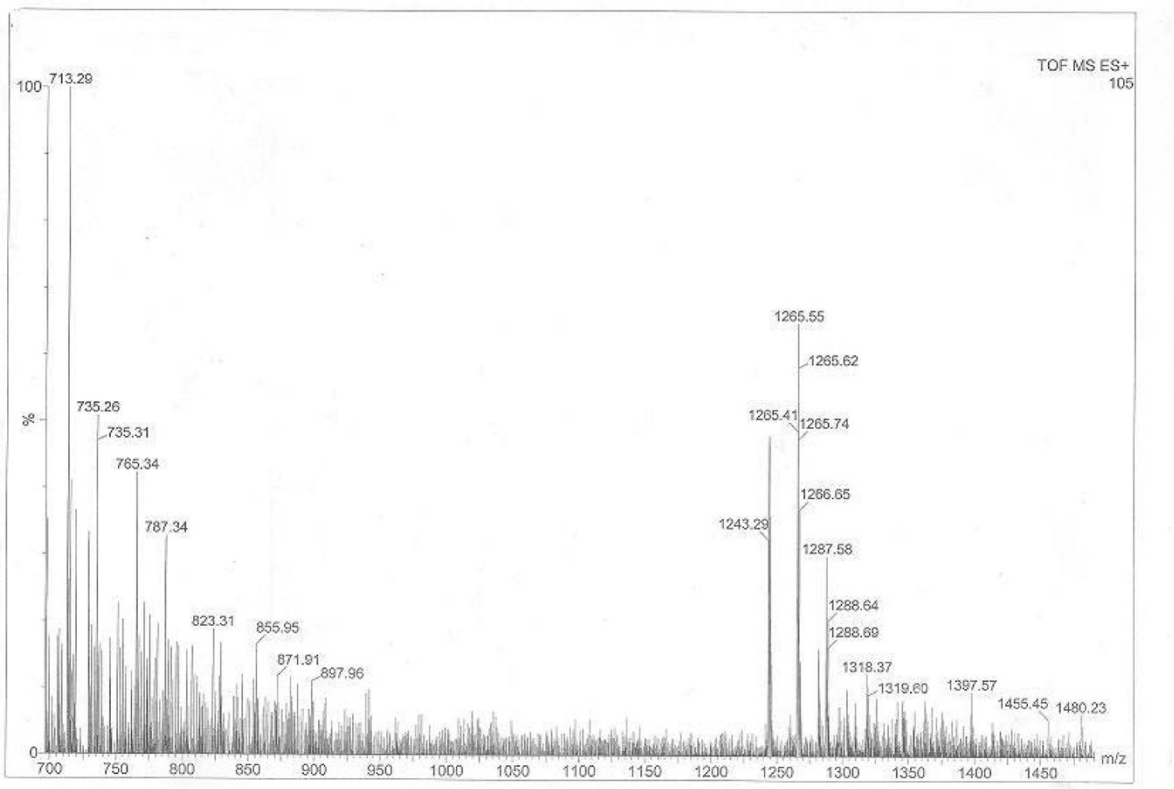

Figure S1: LRMS-ESI+ Mass spectra of the rutin-Cu(II) complex. Complex dissolved in acetonitrile.

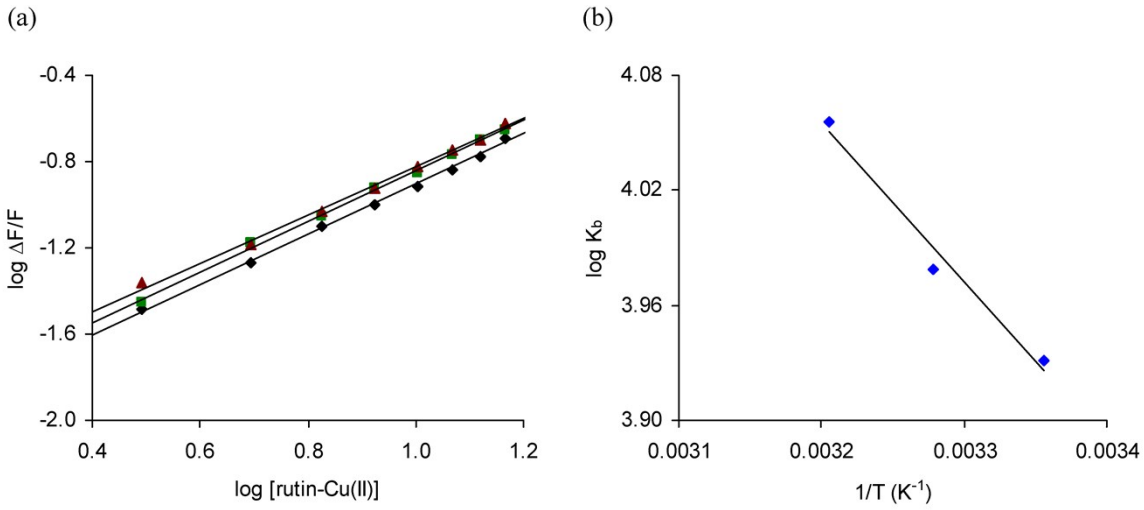

Figure S2: (a) The double-logarithm plots for the interaction of the rutin-Cu(II) complex with EB-ct-DNA at different temperatures and (b) the van't Hoff for the interaction of the complex with EB-ct-DNA. (♦) 298 K;(■) 305 K and (▲) 312 K; λ_{ex}: 480 nm.

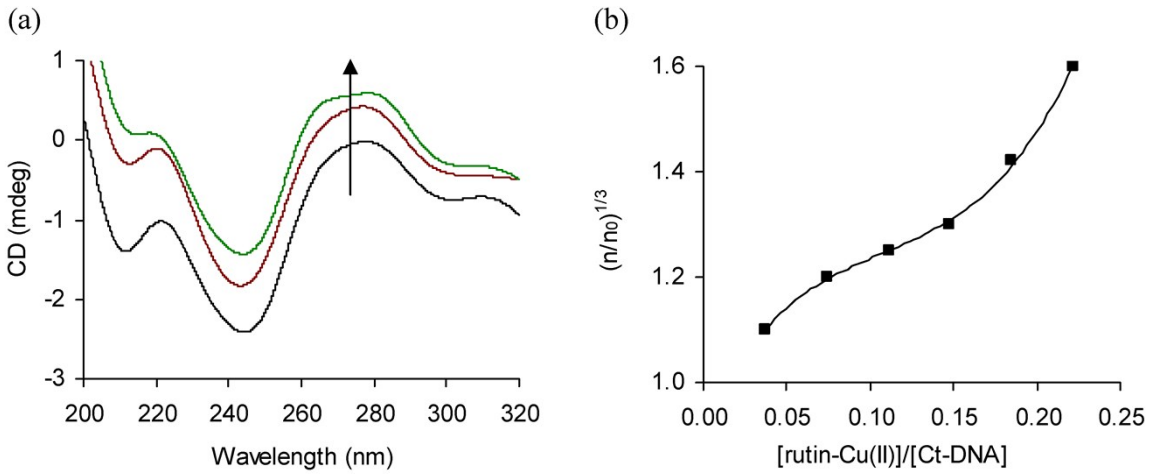

Figure S3: (a) CD spectra of ct-DNA (20 μM) in absence and presence of the rutin-Cu(II) complexes at different molar ratios (0 to 2 μM). (b) Changes in viscosity of ct-DNA (20 μM) after binding with rutin-Cu(II) complex at different molar ratios (0 to 5 μM).

(a)

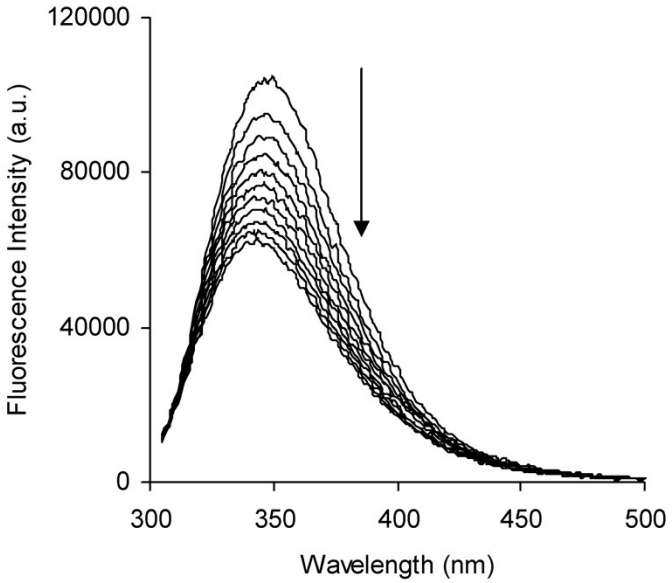

(b)

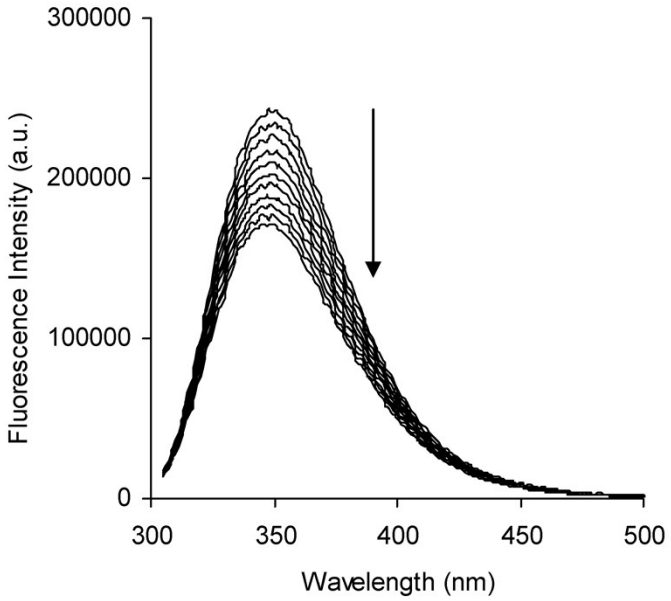

Figure S4: Fluorescence emission spectra of (a) HSA (2 μM) and (b) BSA (2 μM) in absence and presence of rutin (0 to 8 μM) in 20 mM phosphate buffer (pH 7.0) solution at 299 K; λ_{ex}: 295 nm. Arrows indicate the increasing ligand concentration.

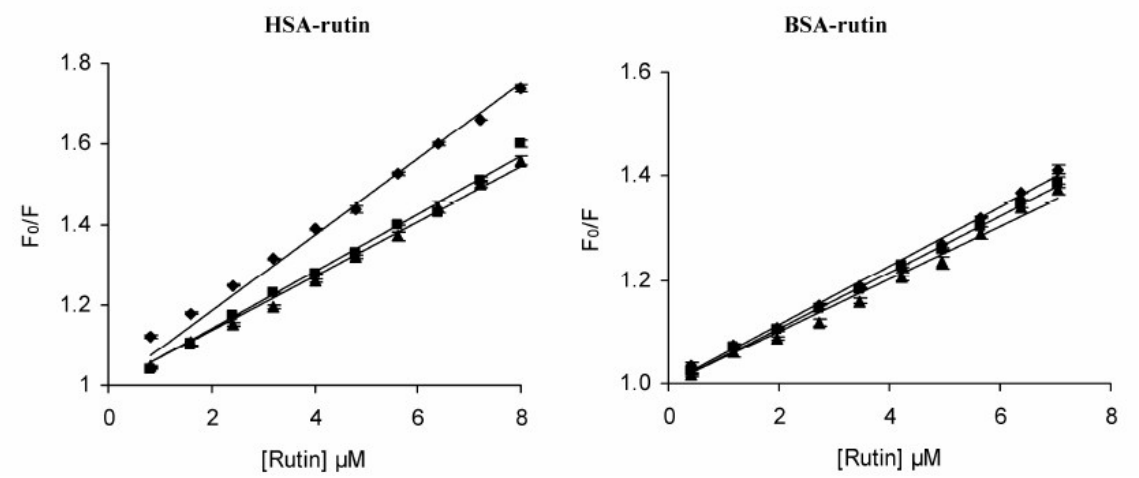

Figure S5: Stern-Volmer plots of HSA and BSA with increasing concentration of quercetin (0 to 8 and 7 µM for HSA and BSA respectively). Inset: The linear range plots of the Stern-Volmer plots. (♦) 299 K;(■) 306 K;(▲) 312 K; λ_{ex} = 295 nm.

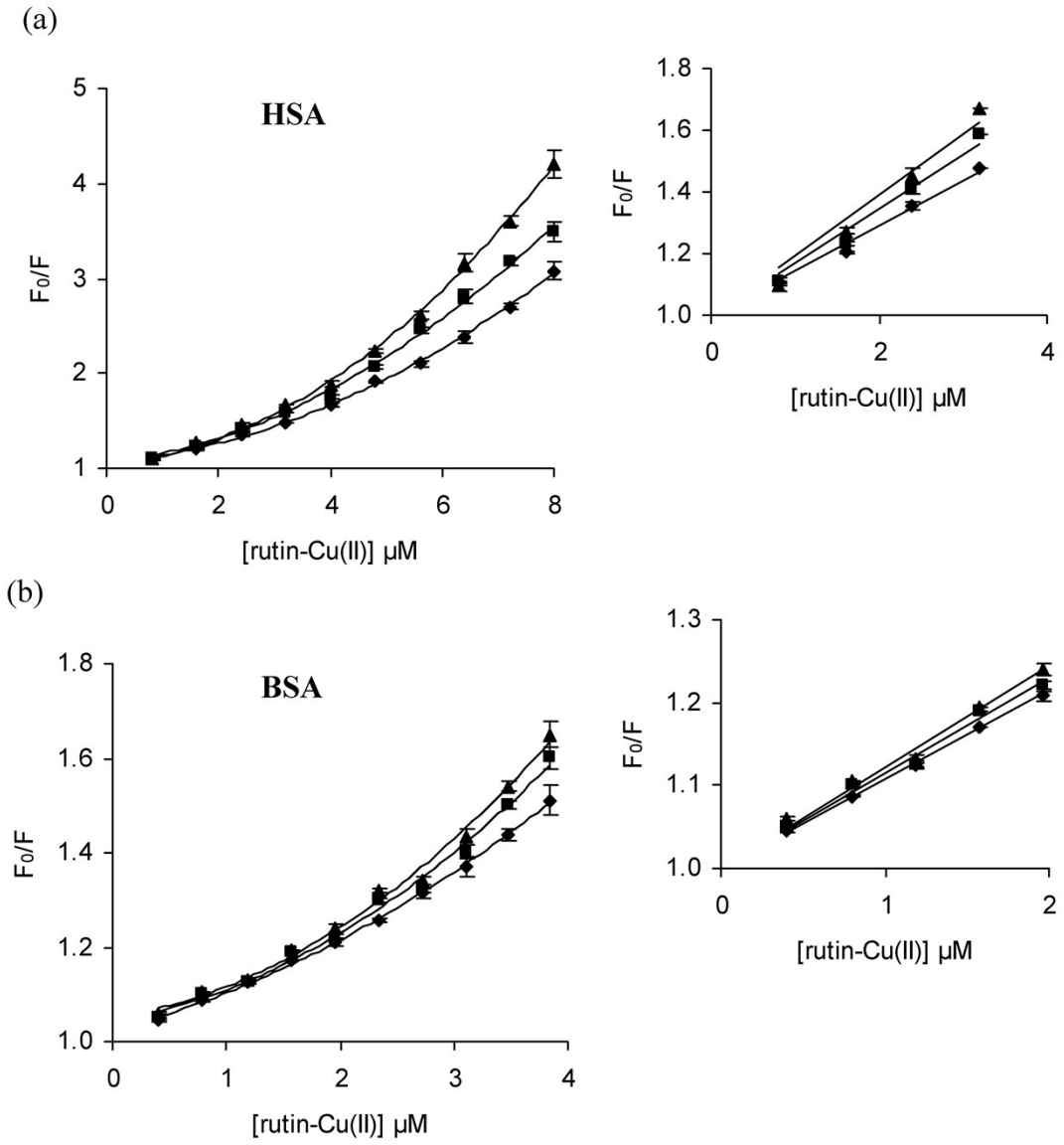

Figure S6: Stern-Volmer plots for the interaction of rutin-Cu(II) complex with (a) HSA and (b) BSA. Inset: The linear range plots. (♦) 299 K; (■) 306 K; (▲) 312 K; λ_{ex} = 295 nm.

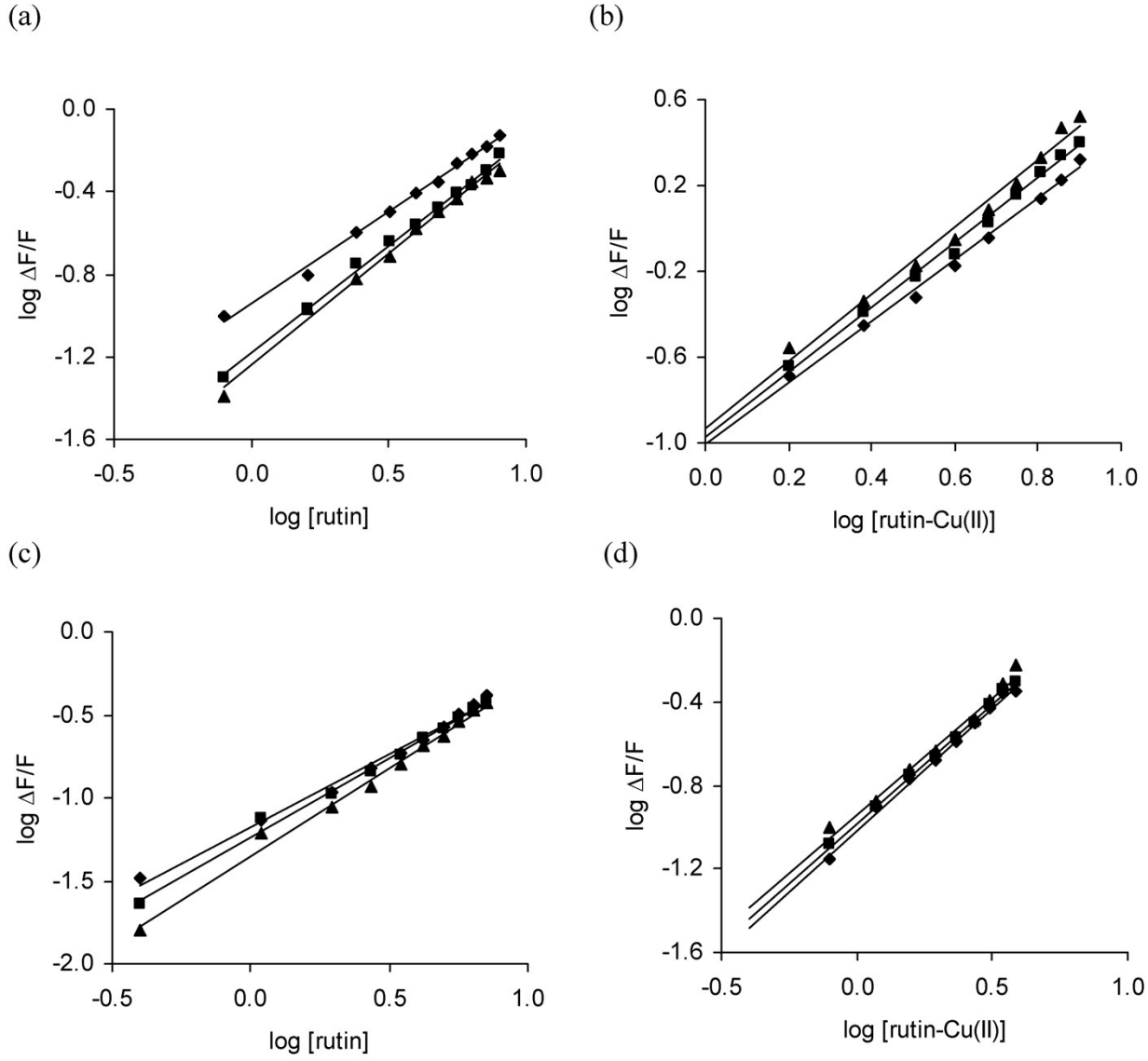

Figure S7: Double-logarithm plot of the interaction of the rutin and rutin-Cu(II) complex with HSA (a), (b) and BSA (c), (d). For rutin interacting with SAs (♦) 299 K;(■) 306 K;(▲) 312 K; For rutin-Cu(II) complex with SAs (▲) 299 K;(■) 306 K;(♦) 312 K λ_{ex} = 295 nm

(a)

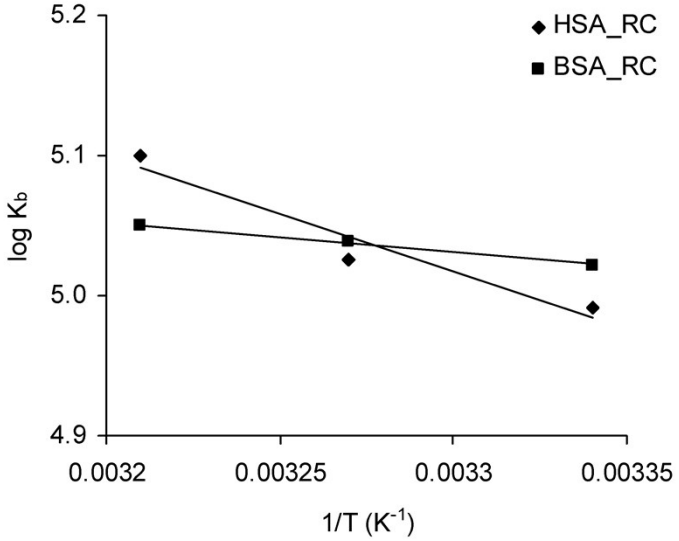

(b)

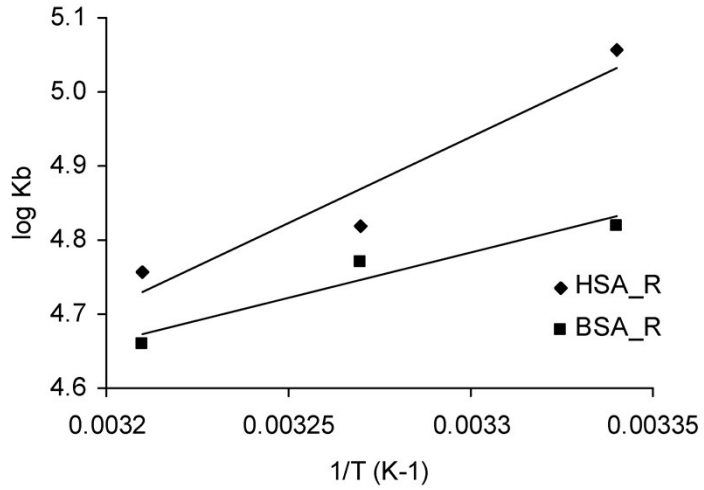

Figure S8: The van't Hoff plot for interactions of rutin-Cu(II) complex (a) and rutin (b) with HSA and BSA in 20 mM phosphate buffer (pH 7.0).

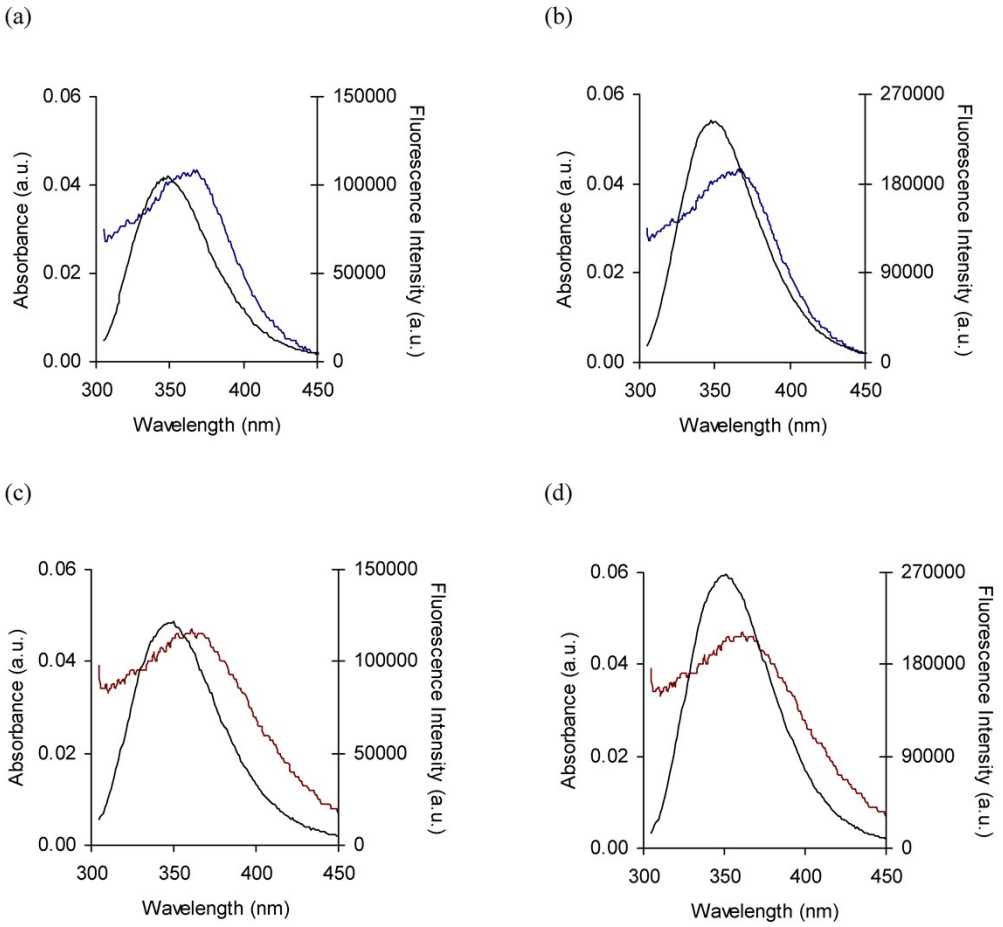

Figure S9: Spectral overlap between the fluorescence emission spectrum of SAs (solid line) and the absorption spectrum of ligands bound with SAs for (a) HSA-rutin, (b) BSA-rutin, (c) HSA-rutin-Cu(II), (d) BSA-rutin-Cu(II) at [ligand]/[protein]=1:1; λ_{ex}: 295 nm and λ_{em}: 347 nm.

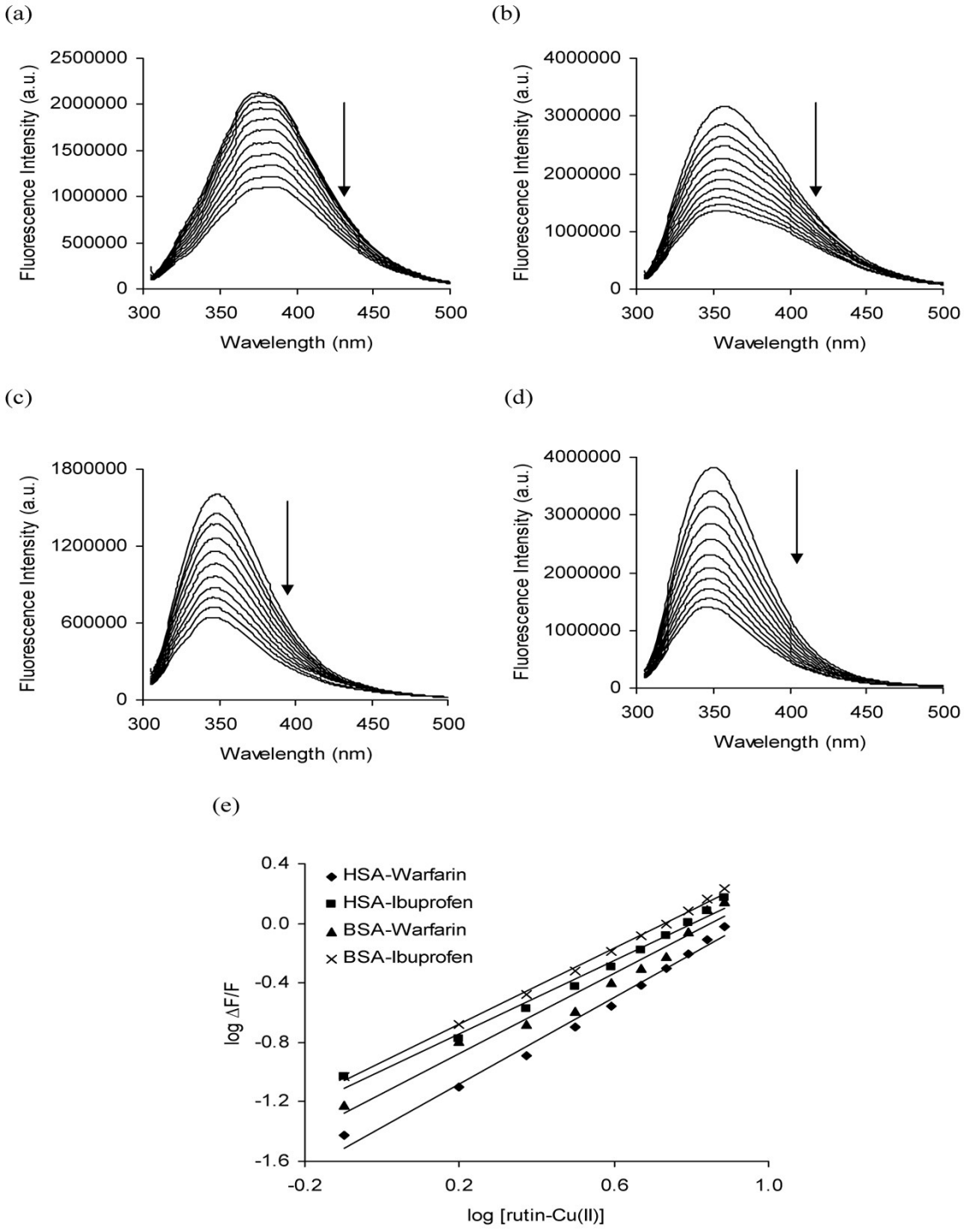

Figure S10. The fluorescence emission spectra of warfarin bound to HSA (a) and BSA (b) with increasing concentration of rutin-Cu(II) complex (0 to 8 μM). The same for ibuprofen bound to HSA (c) and BSA (d). The corresponding binding plots are given in (e). λ_{ex} = 295 nm.

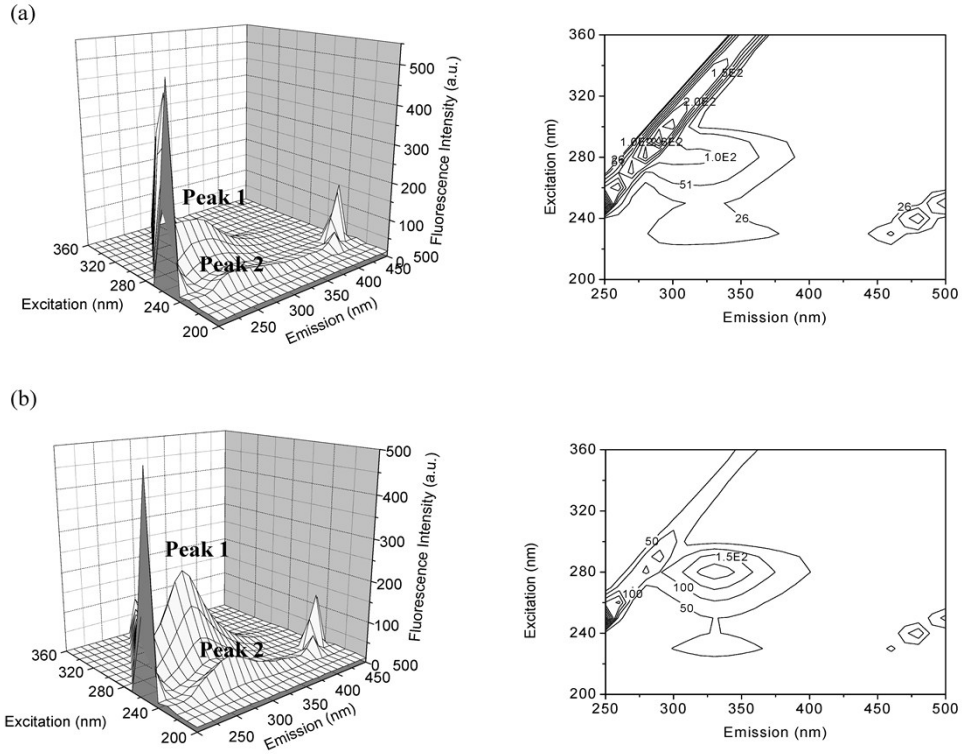

Figure S11: Three-dimensional spectra of HSA (a) and BSA (b) in presence of rutin (25 μM). The contour plots of the corresponding three-dimensional diagrams are provided in the same row of each. [SAs] = 5 μM.

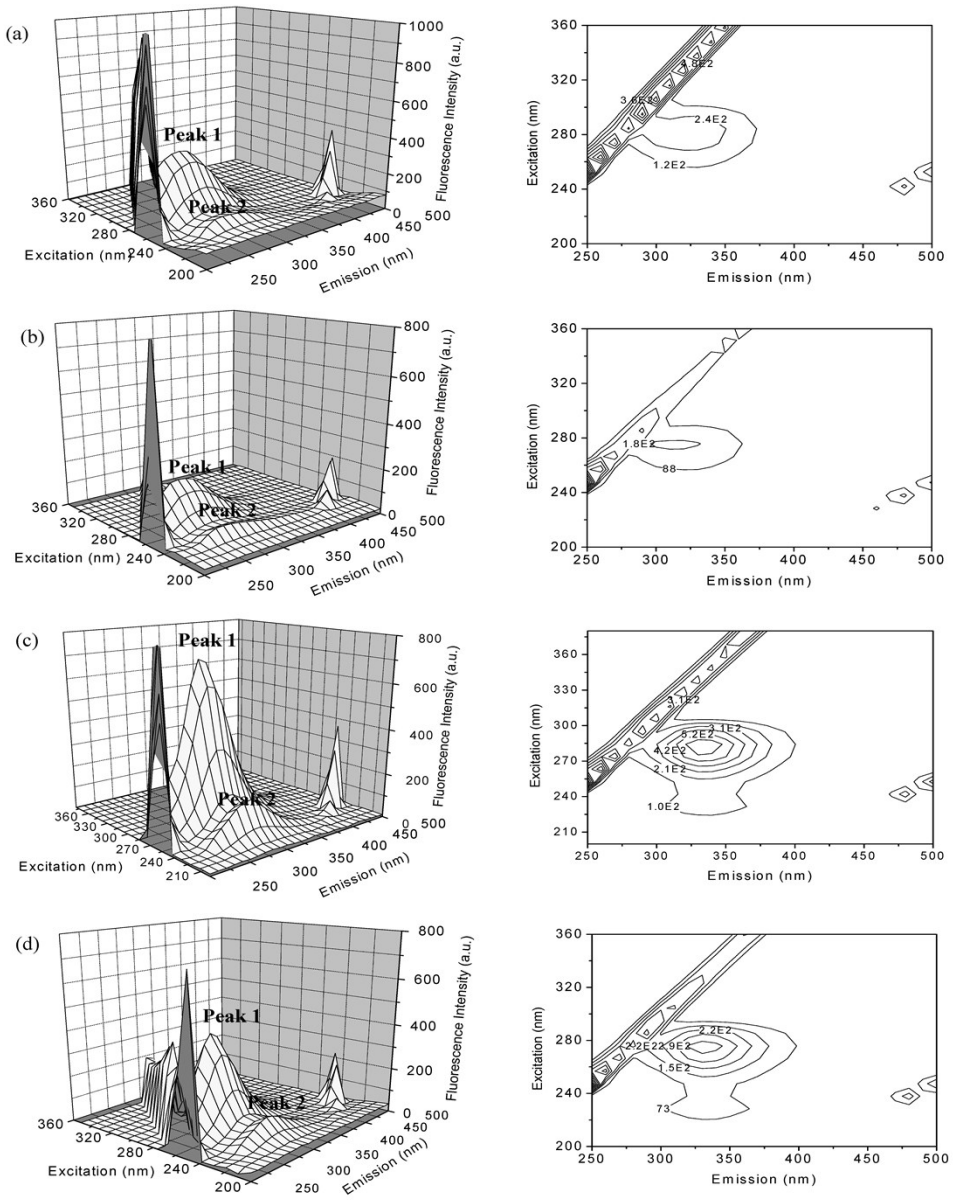

Figure S12: Three-dimensional spectra of HSA (5 μM) in (a) absence and (b) presence of rutin-Cu(II) complex (25 μM). The same for BSA in (c) absence and (d) presence of the copper complex. The contour plots of the corresponding three-dimensional diagrams are provided in the same row of each.

(a)

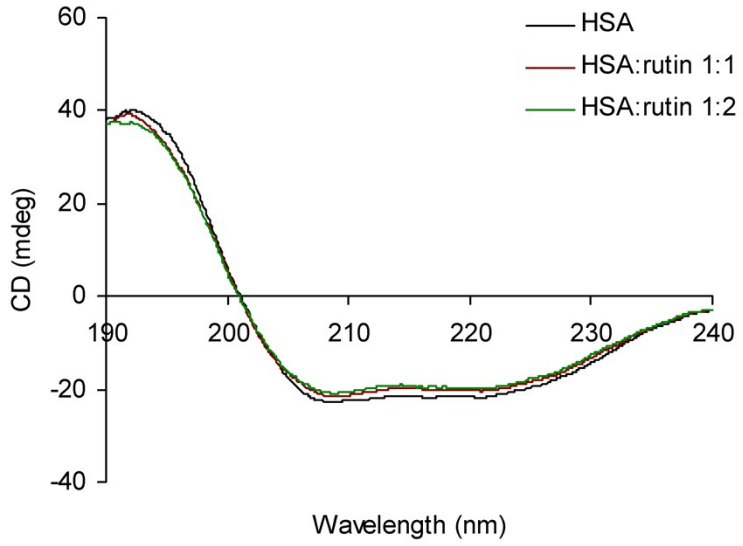

(b)

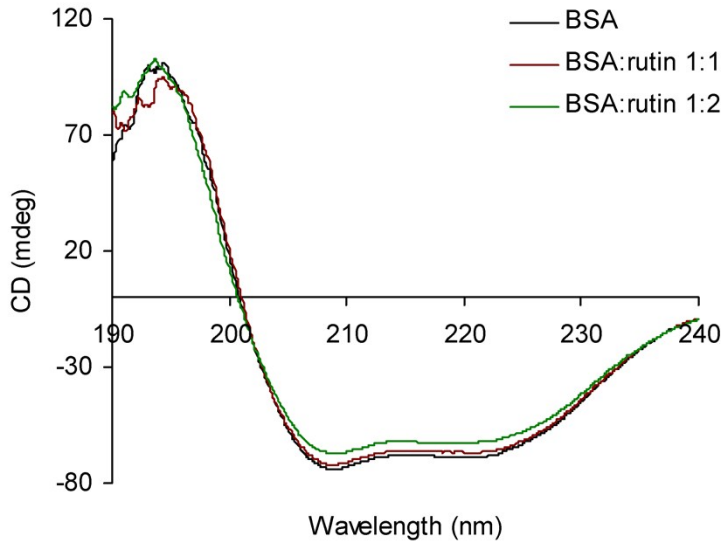

Figure S13: Far CD spectra of HSA + rutin (a) and BSA + rutin (b). Free protein (black line) and SAs:rutin (brown and green lines for 1:1 and 1:2 molar ratios respectively) in both cases. [HSA] = 2 μM and [BSA] = 5 μM.

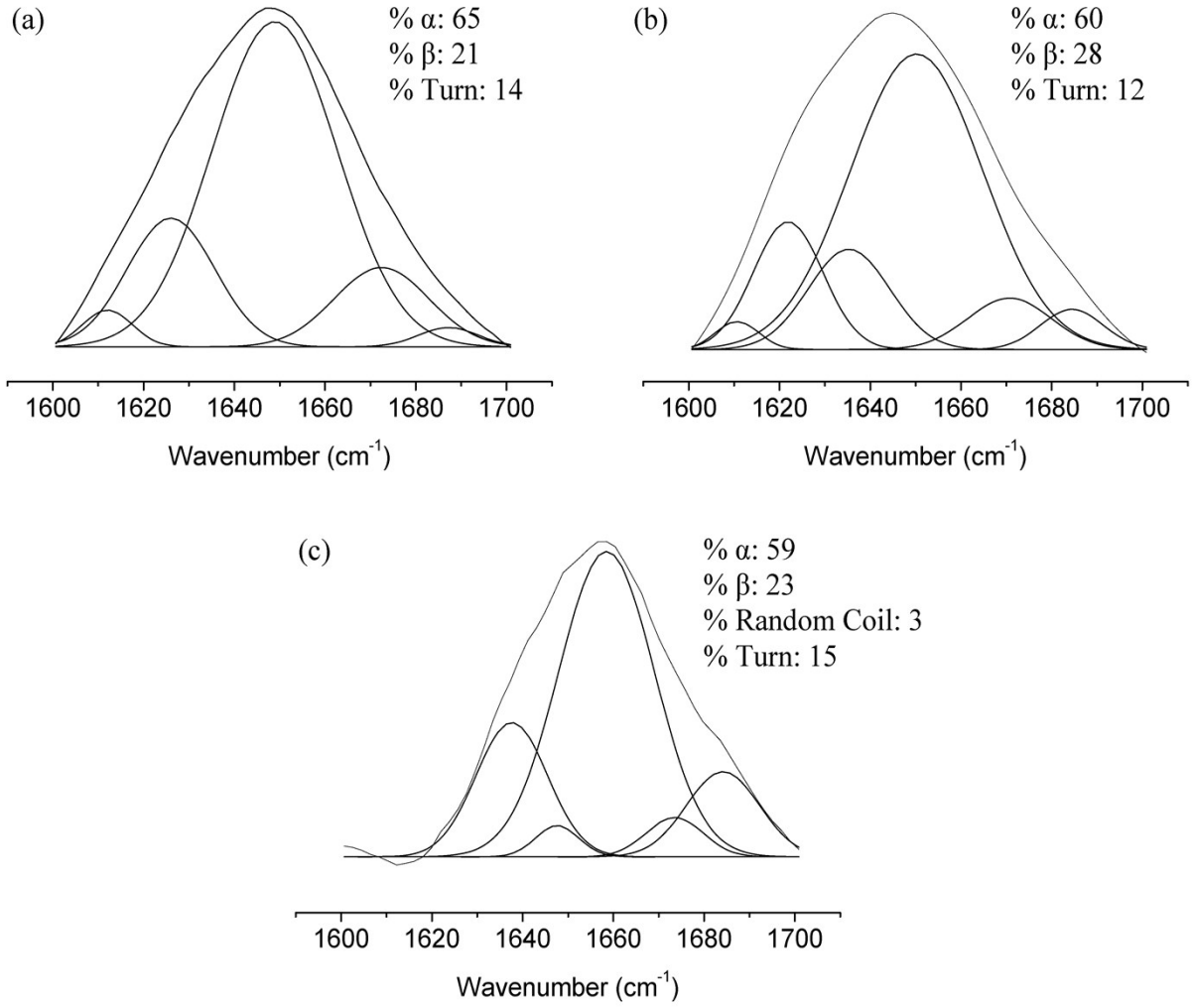

Figure S14: Curve-fitted amide I (1700-1600 cm^{-1}) regions of free HSA (a) and HSA-rutin (b) and HSA-rutin-Cu(II) (c) complexes (molar ratio 1:2) in 20 mM phosphate buffer of pH 7.0.

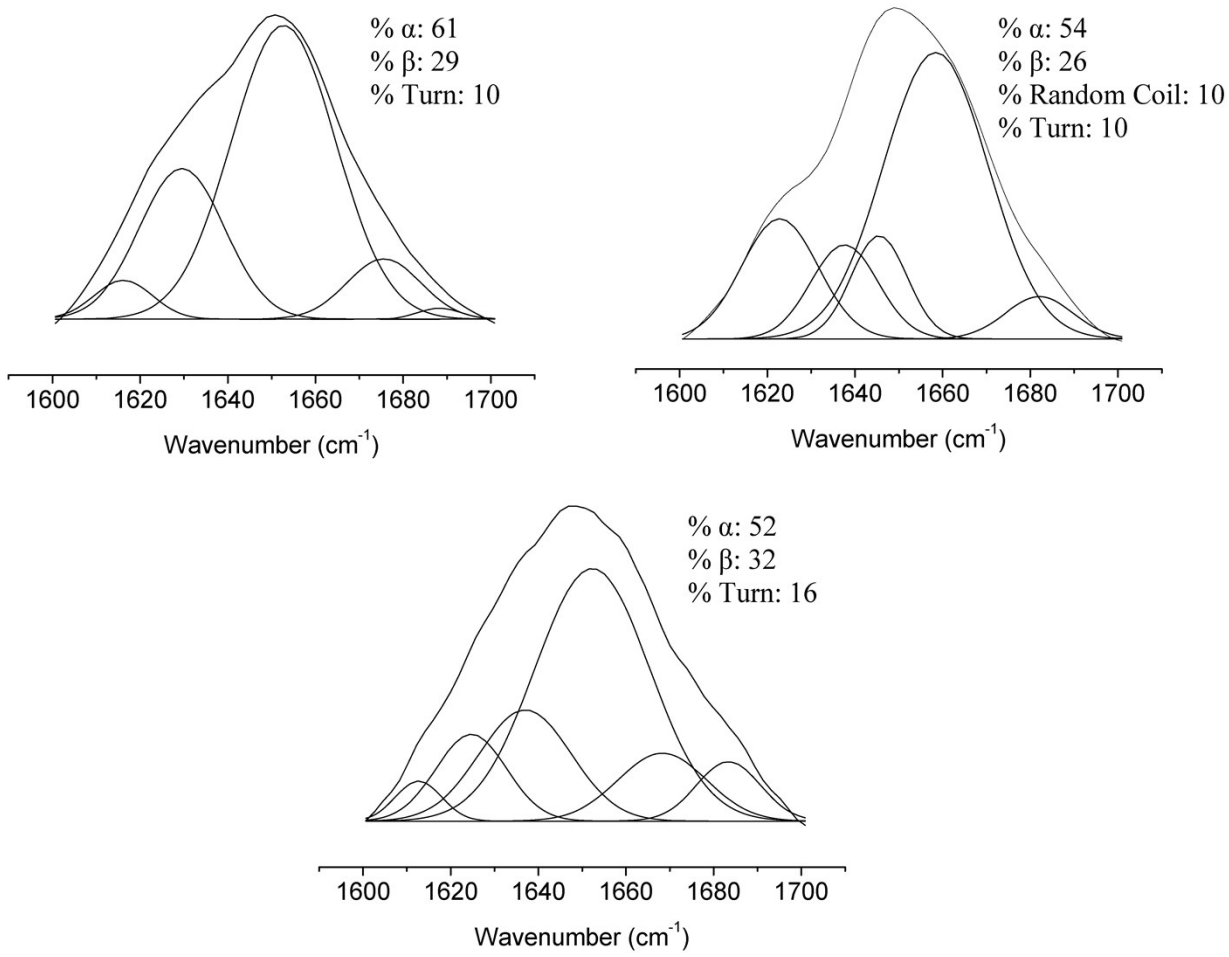

Figure S15: Curve-fitted amide I (1700-1600 cm^{-1}) regions of free BSA (a) and BSA-rutin (b) and BSA-rutin-Cu(II) (c) complexes (molar ratio 1:2) in 20 mM phosphate buffer of pH 7.0.

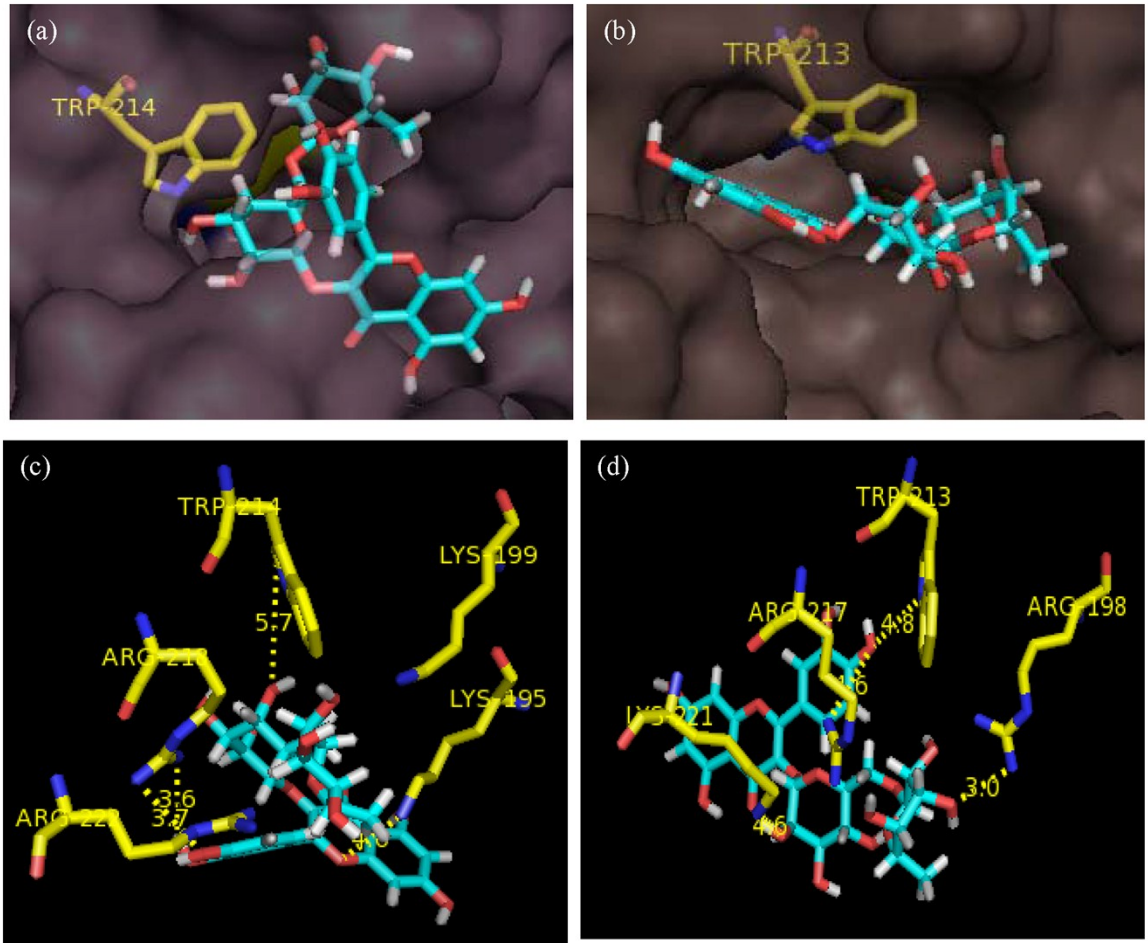

Figure S16: The surface representation of the docked conformations of rutin with HSA (a) and BSA (b); The H-bonding distances of rutin from the interacting residues of HSA (c) and BSA (d).

(a)

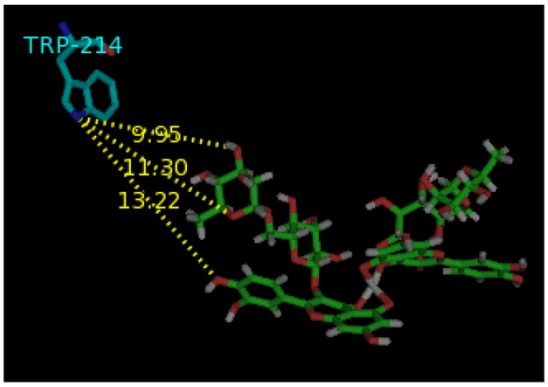

(b)

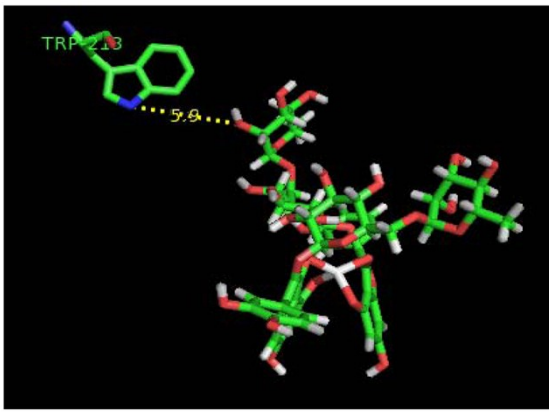

Figure S17: The H-bonding distances of rutin-Cu(II) complex from the Trp 214 and Trp 213 residues of HSA (a) and BSA (b).

Table S1. The quenching parameters for the interaction of the rutin-Cu(II) complex with ct-DNA

Temp.	$10^{-4}\times K_{sv}$ (M^{-1})	$10^{-12}\times K_q$ ($M^{-1}\ s^{-1}$)
25 °C	1.16±0.02 (R^2 = 0.9777)	2.32
32 °C	1.37±0.01 (R^2 = 0.9873)	2.74
38 °C	1.56±0.01 (R^2 = 0.9813)	3.12

Table S2. K_{SV} and K_q values for the binding of the rutin (column 1 and 2) and rutin-Cu(II) complex (column 3 and 4) with HSA and BSA

	Temp.	$10^{-4}\times K_{SV}$ (M^{-1})	$10^{-13}\times K_q$ (M^{-1} s^{-1})	$10^{-5}\times K_{SV}$ (M^{-1})	$10^{-13}\times K_q$ (M^{-1} s^{-1})
HSA	299 K	9.39±0.01 (R^2=0.987)	1.88	1.45±0.02 (R^2=0.965)	2.90
	306K	7.11±0.02 (R^2=0.992)	1.42	1.73±0.03 (R^2=0.968)	3.46
	312 K	6.81±0.01 (R^2=0.995)	1.36	1.95±0.02 (R^2=0.987)	3.90
BSA	299 K	5.66±0.01 (R^2=0.995)	1.13	1.07±0.01 (R^2=0.983)	2.44
	306 K	5.39±0.01 (R^2=0.998)	1.08	1.15±0.01 (R^2=0.982)	2.30
	312 K	5.07±0.02 (R^2=0.986)	1.01	1.22±0.01 (R^2=0.998)	2.14

Table S3. Thermodynamic parameters for the interactions of rutin with HSA and BSA

	Temp.	$\Delta G°$ (kJ mol^{-1})	$\Delta H°$ (kJ mol^{-1})	$\Delta S°$ (J mol^{-1} K^{-1})
HAS/Rutin	299 K	-(28.81±0.06)	-(42.07±2.92)	-(44.31±4.85)
	306 K	-(28.51±0.13)		
	312 K	-(28.24±0.19)		
BSA/Rutin	299 K	-(27.69±0.18)	-(23.29±2.33)	+(14.71±4.95)
	306 K	-(27.79±0.24)		
	312 K	-(27.88±0.29)		

Table S4. The % α-helix data of HSA and BSA after interactions with rutin and rutin-Cu(II) complex

Protein	[Protein]/[ligand]	% α-helix (CD)	% α-helix (FTIR)
HSA/Rutin	1:0	54	65
	1:1	52	63
	1:2	51	60
HSA/Rutin-Cu(II) complex	1:0	54	65
	1:1	52	62
	1:2	50	59
BSA/Rutin	1:0	61	61
	1:1	59	58
	1:2	57	54
BSA/Rutin-Cu(II) complex	1:0	61	61
	1:1	58	57
	1:2	56	52

Table S5. The change in accessible surface area (ΔASA) in $Å^2$ of the interacting residues of HSA (uncomplexed), and their complexes with the rutin-Cu(II)

Residues	Helix	ΔASA ($Å^2$)
LYS 195		-
TRP 214	IIA-h2	-
ARG 218	IIA-h2	35.16
ARG 222	IIA-h2	20.24
GLU 277		5.27
LYS 281		45.62
HIS 288	IIA-h6	34.46
CYS 289	IIA-h6	21.95
GLU 292	IIA-h6	72.01
VAL 293		23.45
GLU 294		44.05
LYS 436	IIIA-h3	14.83
HIS 440	IIIA-h3	9.77
LYS 444	IIIA-h3	26.25
PRO 447	IIIA-h3	23.91

Table S6. The change in accessible surface area (ΔASA) in $Å^2$ of the interacting residues of HSA (uncomplexed), and their complexes with rutin

Residues	Helix	ΔASA ($Å^2$)
LYS 195		71.83
TRP 214	IIA-h2	28.28
ARG 218	IIA-h2	39.59
ARG 222	IIA-h2	34.13
LEU 238	IIA-h3	10.04
ALA 291	IIA-h6	20.4
GLU 292	IIA-h2	33.94
VAL 293		8.11
GLU 294		3.48
ASN 295		12.18
PRO 447	IIIA-h3	10.96
CYS 448	IIIA-h3	19.07
ASP 451	IIIA-h3	21.6
TYR 452	IIIA-h3	20.89

Table S7. The change in accessible surface area (ΔASA) in Å^2 of the interacting residues of BSA (uncomplexed), and their complexes with the rutin-Cu(II)

Residues	Helix	ΔASA (Å^2)
LYS 187		54.81
THR 190		13.71
SER 191	IB-h4	17.95
ARG 194	IB-h4	52.79
ARG 198		24.42
TRP 213	IIA-h2	
ARG 217	IIA-h2	54.52
HIS 287	IIA-h5	11.55
CYS 288	IIA-h5	14.19
ALA 290	IIA-h6	35.18
GLU 291	IIA-h6	99.01
VAL 292	IIA-h6	16.61
GLU 293		56.22
LYS 294		29.72
ARG 435	IIIA-h3	13.32
LYS 439		40.37
GLU 443		60.03
TYR 451	IIIA-h3	29.45

Table S8. The change in accessible surface area (ΔASA) in Å^2 of the interacting residues of BSA (uncomplexed), and their complexes with the rutin

Residues	Helix	ΔASA (Å^2)
ARG 194		63.97
ARG 198		21.51
TRP 213	IIA-h2	9.92
ARG 217	IIA-h2	68.94
ALA 290	IIA-h6	28.73
GLU 291	IIA-h6	33.74
LYS 294		35.33
GLU 339		18.67
VAL 342		23.22
GLU 443		40.04
PRO 446	IIIA-h3	14.73
ASP 450	IIIA-h3	36.01